INORGANIC CHEMISTRY FRONTIERS

RESEARCH ARTICLE

View Article Online
View Journal | View Issue

Cite this: *Inorg. Chem. Front.*, 2024, **11**, 7545

Dinuclear platinum(II) complexes emitting through TADF: new ligand design to minimise aggregation and the S_1–T_1 energy gap†

Piotr Pander, *‡[a,b] Yana M. Dikova, ‡[c] Emma V. Puttock [c] and J. A. Gareth Williams *[c]

Received 14th August 2024,
Accepted 13th September 2024

DOI: 10.1039/d4qi02069c

rsc.li/frontiers-inorganic

Dinuclear platinum(II) complexes of a new, ditopic, bis-tridentate *NCN–NCN*-coordinating ligand, appended with four mesityl groups, are reported. The high radiative rate constants and correspondingly efficient luminescence of the complexes involves thermally activated delayed fluorescence (TADF), thanks to a near-zero energy gap between the S_1 and T_1 states. The mesityl groups also serve to hinder the aggregation that was detrimental to electroluminescence efficiency in previous studies, allowing a ~4-fold increase in OLED efficiency to be achieved (*i.e.* from 2.3% previously to 10% in this work). Oxidation of one of the Pt(II) complexes led to a dinuclear Pt(IV) complex of unprecedented structure.

Introduction

Organoplatinum(II) complexes are widely used as the luminophore or sensitizer in diverse applications, often complementing their iridium(III) counterparts.[1–3] Important uses include bioimaging,[4–9] photodynamic therapy,[10] photocatalysis,[11–14] and organic light-emitting diodes (OLEDs).[15–18] The luminescence displayed by such complexes is normally considered phosphorescence, whereby the high spin–orbit coupling associated with the heavy metal relaxes the spin selection rule, accelerating the rate of the otherwise forbidden $T_1 \rightarrow S_0$ process.[2,19] However, recent findings by some of the present authors have revealed that another mechanism may be at work in at least some such complexes, involving thermally activated delayed fluorescence (TADF).[20–22] Dinuclear Pt(II) complexes of ditopic ligands featuring a pyrimidine bridge were found to have a small energy gap ΔE_{ST} between the lowest singlet S_1 and triplet T_1 excited states.[21] It leads to a shortening of the decay lifetime by thermal activation of T_1 to S_1 and subsequent emission through the allowed $S_1 \rightarrow S_0$ transition (*i.e.*, following the TADF model).[23,24] A similar phenomenon has since been observed by others in a mononuclear Pt(II) complex,[25] and the future discovery of many further examples seems likely. While preparing this manuscript, another work reporting both mono- and dinuclear Pt(II) complexes showing TADF has been published, reporting high OLED efficiency and low efficiency roll-off.[26] This further underscores the potential advantages that TADF complexes of this metal offer.

In the present work, we took our original ligand design and appended it with four 2,4,6-trimethylphenyl (mesityl) groups, with a view to improving the solubility of the resulting complex and reducing aggregation. We also show how this seemingly otherwise insignificant structural change leads to a reduction in ΔE_{ST}, which in turn enhances the TADF contribution to emission and substantially improves performance.

Results and discussion

Synthesis

The new ditopic *NCN–NCN* proligand H_2L (compound **4** in Scheme 1) was prepared by a sequence of Pd-catalysed cross-coupling reactions from readily obtainable starting materials; full experimental details and the characterisation of new compounds are given in the ESI.† Compound H_2L was platinated using K_2PtCl_4 in acetic acid to give the dinuclear complex $L(Pt–Cl)_2$ (**5**), from which the iodo derivative $L(Pt–I)_2$ (**6**) was prepared by metathesis of the monodentate ligand upon treatment with $Ag(SO_3CF_3)$ followed by KI. We were unable to obtain crystals of **5** or **6** of sufficient quality for an X-ray diffraction study, but the oxidation of **5** with $PhICl_2$ led cleanly to

[a]*Faculty of Chemistry, Silesian University of Technology, M. Strzody 9, 44-100 Gliwice, Poland. E-mail: piotr.pander@polsl.pl*
[b]*Centre for Organic and Nanohybrid Electronics, Silesian University of Technology, Konarskiego 22B, 44-100 Gliwice, Poland*
[c]*Department of Chemistry, Durham University, South Road, Durham, DH1 3LE, UK*

†Electronic supplementary information (ESI) available: Synthetic details and characterisation of new materials; X-ray diffraction and crystal data; further information on the equipment and methods for theory, photophysical characterisation, and OLED devices. CCDC 2365020. For ESI and crystallographic data in CIF or other electronic format see DOI: https://doi.org/10.1039/d4qi02069c

‡These authors contributed equally to the experimental work.

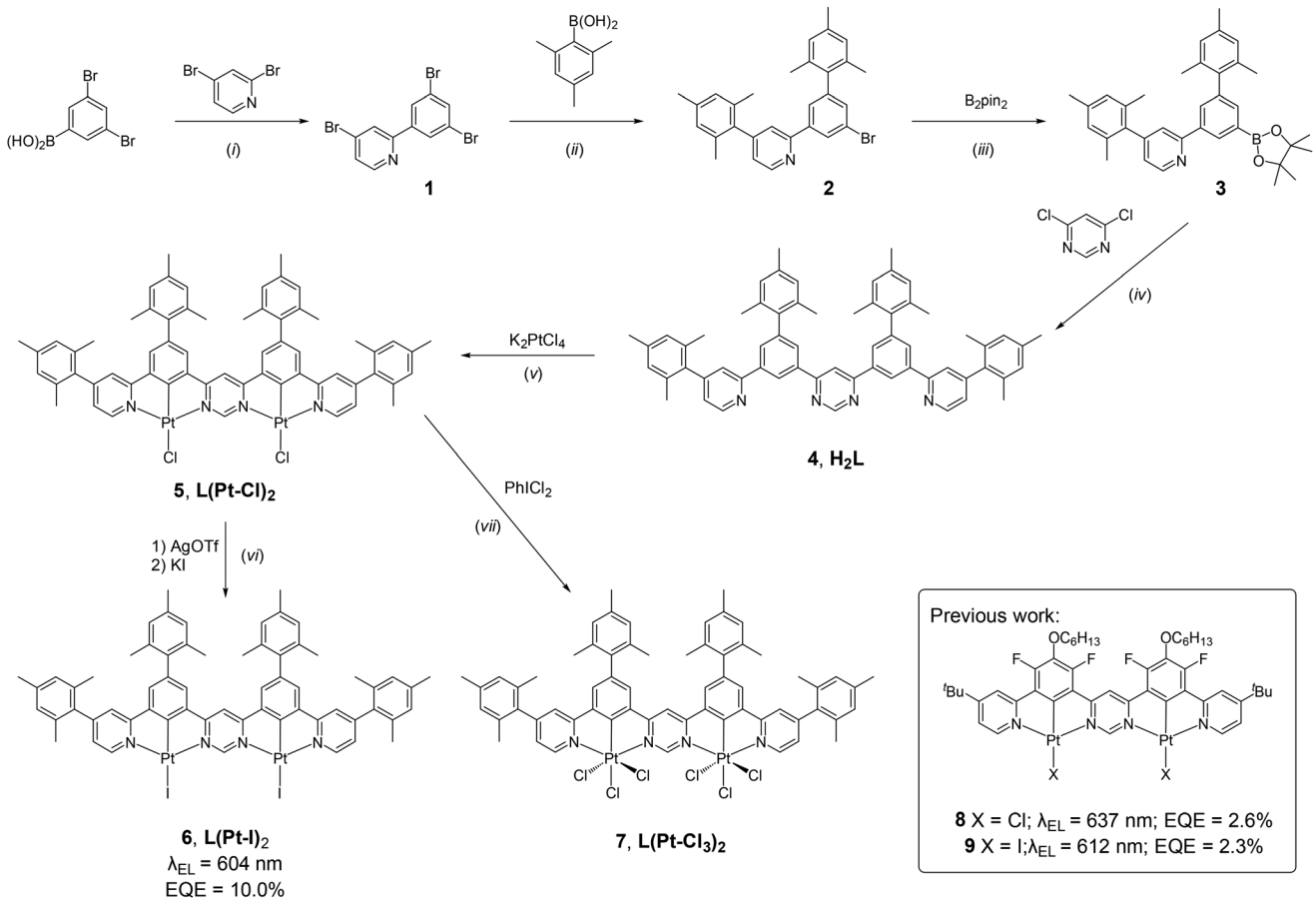

Scheme 1 Synthetic procedure for complexes **5**, **6** and **7**: (i) toluene/EtOH/H_2O (2 : 1 : 1 v/v), $Pd(PPh_3)_4$, Na_2CO_3, 70 °C (2 h) → 90 °C (18 h), 35%; (ii) toluene, $Pd(PPh_3)_4$, Cs_2CO_3, 90 °C (18 h), 67%; (iii) dioxane, $Pd(dppf)Cl_2{\cdot}CH_2Cl_2$, KOAc, 90 °C (18 h); (iv) toluene, $Pd(PPh_3)_4$, Cs_2CO_3, 90 °C (18 h), 35%; (v) AcOH, reflux, 65%; (vi) step 1: acetone, RT (1.5 h); step 2: RT (2 h); 67%; (vii) $CHCl_3$, RT (18 h), 78%. Inset: The previously studied complexes **8** and **9** incorporating a related *NCN–NCN*-coordinating ligand.

L(Pt–Cl_3)$_2$ (**7**), a dinuclear Pt(IV) complex of unprecedented structure that was amenable to crystallography. Although the thrust of the current work is the Pt(II) systems, there is growing interest in the less widely explored +4 oxidation state,[27,28] and **7** represents an interesting structure in that context for future elaboration by replacement of the chloride ligands.[29] Here, it offers insight into the likely structures of **5** and **6**. The structure (Fig. 1) shows the two Pt centres in very similar pseudo-octahedral environments, each bound to an *NCN* unit with three chlorides completing the coordination sphere. The torsion angles between the mesityl and phenyl rings are in the range 69 ± 3° and, between the pyridyl and mesityl rings, 69 ± 5°. These angles are a little less than that of 80° in the related mesityl-appended *NCHN* proligand,[30] suggesting a slightly greater degree of conjugation across the rings upon complexation, attenuating the steric preference for orthogonality.

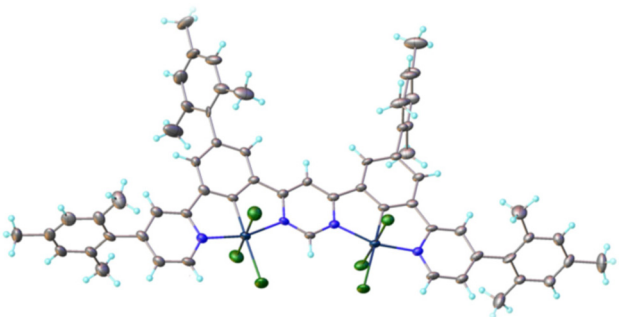

Fig. 1 The molecular structure of the dinuclear Pt(IV) complex L(Pt–Cl_3)$_2$, **7**.

DFT and TD-DFT calculations

The excited states in **5** and **6** were probed by DFT/TD-DFT at the B3LYP/def2-SVP level of theory using ORCA 5.0.3,[31,32] and by quasi-degenerate perturbation theory (QDPT).[33,34] The optimised T_1 geometries (Fig. 2) show torsions between the plane of the *NCN–NCN* unit and the pendent mesityl rings that are similar to those observed experimentally in the Pt(IV) complex (atomic coordinates for T_1 and S_0 are given as separate ESI†). The mesityl groups thus form a congested shield around the complex, which is expected to inhibit intermolecular interactions between *NCN–NCN* planes.

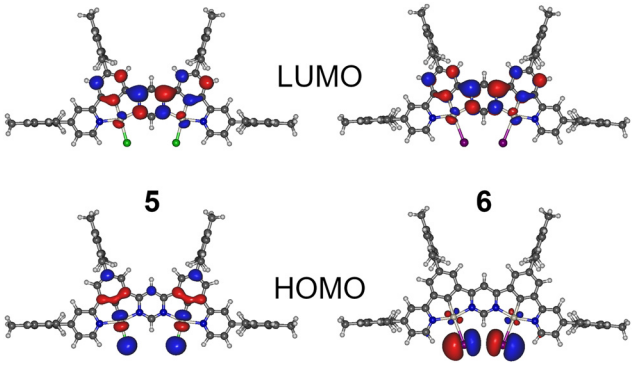

Fig. 2 HOMO and LUMO of complexes **5** and **6** calculated using the B3LYP/def2-SVP//B3LYP/def2-TZVP level of theory.

The frontier molecular orbital isosurfaces of **5** and **6** (Fig. 2) resemble those of **8** and **9**,[21,22] with the LUMO distributed over the pyrimidine linker and the neighbouring benzene rings, but also including a small admixture of d orbitals from both Pt(II) centres. The HOMO comprises d orbitals of both the Pt centres and p orbitals of their respective monodentate halide ligands. For **6**, there are no significant contributions from other parts of the molecule, such that the degree of HOMO–LUMO overlap is small. In **5**, the HOMO includes additional contributions from π orbitals of the organic ligand, which serves to increase the HOMO–LUMO overlap. In both complexes, the S_1 and T_1 are associated mainly with the HOMO → LUMO transition, and thus may be classed as predominantly MXLCT or metal-halogen-to-ligand charge-transfer in character. Complex **6** appears to display a stronger MXLCT character of the excited state, while **5** shows a rather MXLCT + LC (LC – ligand-centred) character due to a clear contribution of the *NCN–NCN* ligand to HOMO.

When spin–orbit coupling (SOC) is included in the calculations, excited states of predominantly triplet or singlet nature are identified (Fig. S4.1, Tables S4.1 and S4.2†). The lowest triplet state splits into three closely separated levels, the separation between the first and third, ΔE_{1-3}, being the zero-field splitting (ZFS). Values of 2 meV (13 cm^{-1}) and 15 meV (119 cm^{-1}) are calculated for **5** and **6** respectively. In **5**, state 7 is the first excited state with predominant singlet character (68%; states 4–6 are associated with T_2); thus $\Delta E_{ST} = \Delta E_{1-7}$, which is calculated to be 291 meV (2345 cm^{-1}). For **6**, the first predominantly singlet excited state (81.4%) is state 4, and $\Delta E_{ST} = \Delta E_{1-4} = 19$ meV (149 cm^{-1}). The trend to smaller ΔE_{ST} upon changing X from Cl to I is consistent with that observed previously for **8** and **9**.

Solution-state photophysics

The solvent of choice for photophysical measurements is toluene (PhMe) (based on **9** having previously shown the highest radiative rate in this solvent[22]). Here, we studied **6** in toluene, but **5** has poorer solubility and intermolecular interactions suppress its emission leading to a lower Φ_{PL}. We believe that the larger diameter of the X = I as compared to X = Cl hinders close π···π and Pt···Pt intermolecular interactions, leading to the better overall solubility of **6**. This is in line with our previous work where the X = I auxiliary ligand was found to disrupt aggregation of the closely related mono-Pt(II) complexes of the Pt(*NCN*)-X type.[35] The full characterisation of **5** was therefore performed in chlorobenzene (PhCl), where such interactions were essentially absent.§¶ There is substantial overlap between the photoluminescence (PL) spectrum and the lowest-energy absorption band in both complexes (Fig. 3) – a clear indication that the PL originates not from the lowest-energy T_1 state but rather from a higher state, and a strong clue for the involvement of TADF.

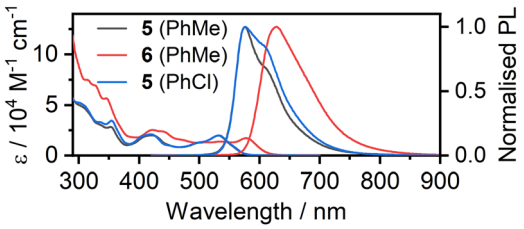

Fig. 3 Absorption and photoluminescence spectra of **5** and **6** in dilute ($c = 10^{-5}$ M) toluene (PhMe) and (for **5**) chlorobenzene (PhCl) solutions.§¶.

The PL spectrum of **6** is very similar to that of the analogous complex **9** (λ_{max}^{PL} = 627 and 628 nm respectively),[22] but the emission spectrum of **5** (λ_{max}^{PL} = 576 nm) is drastically different from that of **8** (λ_{max}^{PL} = 617 nm), Fig. 4. The difference between the PL of **5** and **8** in chlorobenzene can be attributed to a significantly smaller ΔE_{ST} in the former with TADF dominating the spectrum at RT as opposed to **8** with phosphorescence being the dominant component. As the PL onsets are similar in either case, the S_1 energy is likely comparable in both complexes, but the structural differences between the two luminophores lead to a higher T_1 energy in **5** (Table S5.2†).

The PL spectra of the complexes in solution are sensitive to temperature (Fig. S5.1 and S5.2†), in line with the TADF mechanism. For **5** in PhCl, the interplay between phosphorescence and TADF at intermediate temperatures is evident, as in **8**. For **6**, however, the PL spectrum blue shifts very slightly at lower temperatures, indicating a visible influence of suppressed molecular motion. Even at 160 K, there is no evidence of phosphorescence (in stark contrast to the behaviour of **9** for example), suggesting that ΔE_{ST} in **6** is very small indeed, with TADF consequently predominating even at low temperatures.

Complexes **5** and **6** display unusually large radiative decay rate constants k_r for platinum(II) complexes: τ = 0.34 μs, Φ_{PL} =

§A slight difference between the PL spectra of **5** in toluene and chlorobenzene can be ascribed to a variation in the ΔE_{ST}, in line with the previous report of complex **8**.[21] Here, **5** displays a larger ΔE_{ST} in the higher polarity chlorobenzene than in toluene, leading to a visible phosphorescence contribution in chlorobenzene, manifest on the low-energy side of the spectrum.

¶Complex **7** does not show any detectable emission, as expected based on earlier studies.[28,29] The absorption spectrum of **7** is included in the ESI for completeness (Fig. S5.3†).

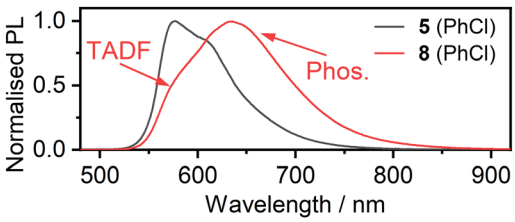

Fig. 4 Comparison of photoluminescence spectra of compounds **5** and **8** recorded in dilute PhCl.

0.11, $k_r = 3.3 \times 10^5\ s^{-1}$ for **5** in PhMe [$\tau = 2.1$ μs, $\Phi_{PL} = 0.45$, $k_r = 2.1 \times 10^5\ s^{-1}$ in PhCl]; $\tau = 0.40$ μs, $\Phi_{PL} = 0.23$, $k_r = 5.7 \times 10^5\ s^{-1}$ for **6** in PhMe.‖ The k_r values are significantly higher than for **8** and **9** (Table S5.1†), suggesting more efficient TADF. We use the method of Strickler and Berg[36] to estimate the singlet-state radiative rate constants k_r^S and $f(S_1 \rightarrow S_0)$ oscillator strengths, from the lowest energy absorption bands.[37,38] For **5** in PhCl, $k_r^S = 5.3 \times 10^7\ s^{-1}$ and $f(S_1 \rightarrow S_0) = 0.12$; corresponding values for **6** in PhMe are $3.3 \times 10^7\ s^{-1}$ and 0.09. The values are two orders of magnitude higher than the experimental values, showing (as expected) that the emission is not fluorescence, but rather pointing to the likely involvement of TADF.

Solid-state photophysics

More conclusive evidence of a TADF mechanism comes from the temperature dependence of the complexes' PL spectra in a dilute polystyrene (PS) film, over the range 295–80 K (Fig. 5). The spectra display a clear change, shifting to the red as the temperature decreases, from which it is apparent that TADF dominates at 295 K, while phosphorescence from the lower-energy T_1 state dominates at 80 K. The evolution of the spectra correlates with a change in the radiative lifetime (Fig. 6, Fig. S5.4 and S5.5†). Fitting of the lifetime data of **6** to an established Boltzmann-based expression (eqn (S2)†) gives a natural fluorescence lifetime $\tau_0 \approx 32$ ns, phosphorescence lifetime $\tau_{PH} \approx 13$ μs, and $\Delta E_{ST} \approx 66$ meV, not dissimilar to the value calculated by TD-DFT. The k_r^S figures for both complexes ($\sim 10^7\ s^{-1}$) are in good agreement with the estimates obtained using the Strickler–Berg method. It is striking that the radiative lifetime at 295 K is an order of magnitude shorter than at 80 K thanks to the involvement of TADF, underscoring how TADF can benefit Pt(II) complexes despite the heavy atom effect that might otherwise be expected to funnel emission through phosphorescence.

OLED devices

Owing to the good PL properties of **6** and its low susceptibility to aggregative quenching (in contrast to **5**), it was tested as an emitter in a solution-processed organic light-emitting diode (OLED). Three pairs of device architectures (Tables S6.1 and S6.3†) were trialled to optimise the efficiency: Devs 1, 3, and 5 at 3% w/w loading of the complex in the host, and Devs 2, 4, and 6 at 5%, to probe the effect of concentration. The pair of devices 1 and 2 use a simple structure with a relatively thick TCTA:PO-T2T host emissive layer.[39] Devices 3 and 4 feature a mCP:PO-T2T host. Devices 5 and 6 employ a mCP:PBD host with a poly(vinyl-carbazole) hole-transporting and electron-blocking layer (as previously used with **9** and hence serving as a reference[22]). The OLED data are presented in Fig. 7, Fig. S6.1–S6.8 and Table S6.1.†

Comparison of Devices 5 and 6 with those reported previously using **9** shows that the use of the new complex leads to a ~4-fold higher EQE (up to 10%) than complex **9**, and a ~2–4-fold higher luminance (up to 8700 cd m^{-2}). Although several factors may have contributed to this result, the main one appears to be suppression of emitter aggregation in the solid state by the mesityl substituents. This effect can be identified from a comparison of the respective EL spectra (Fig. 8). Despite identical emitter loading and OLED structure, Device 6 displays a visibly narrower EL spectrum, lacking the long wavelength tail >700 nm that the previously reported Device 7

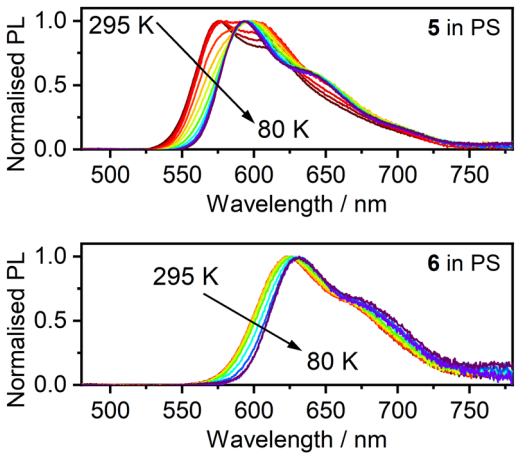

Fig. 5 PL spectra of **5** and **6** in polystyrene dispersion (c = 0.2% w/w) over the temperature range indicated.

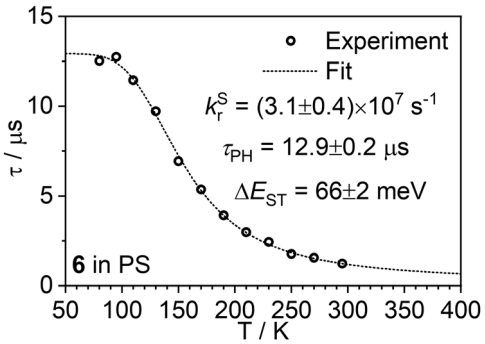

Fig. 6 Variation of the PL decay lifetime τ of **6** as a function of temperature T.

‖ k_r is estimated from the lifetime and quantum yield, assuming unit population of the emissive state, where $k_r = \Phi/\tau$. The quoted τ and Φ values were measured in deoxygenated solution at 295 K.

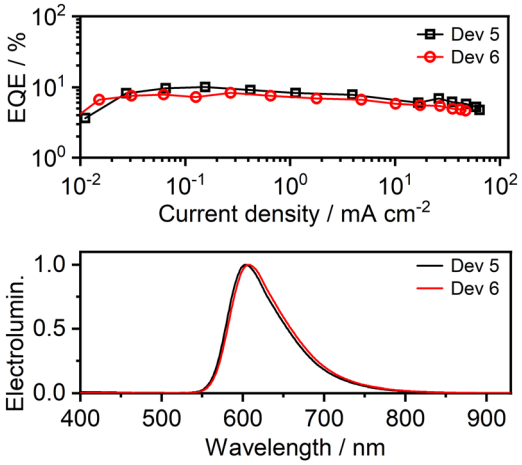

Fig. 7 Characteristics of OLEDs **5** and **6**: (top) External quantum efficiency (EQE); (bottom) EL spectra.

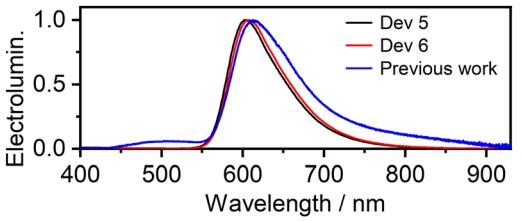

Fig. 8 Comparison of the EL spectra of OLEDs **5** and **6** with the EL spectrum of OLED **7** (using complex **9**) from previous work.[22]

shows (using complex **9**). That tail is due to dimeric or oligomeric species formed through aggregation; it is detrimental both to the overall OLED EQE and to colour purity.** Thus, the encumbered molecular design is successful in promoting efficiency in OLEDs using dinuclear Pt(II) TADF emitters.

Conclusions

In conclusion, the design of ligand **4** – featuring a ditopic *NCN–NCN* core decorated with four mesityl units – successfully limits aggregation of complex **6**, inhibiting the detrimental effect on EL in an OLED. Complex **6** is highly soluble in toluene and other solvents and displays a lower susceptibility to aggregation in the solid state than the previously reported complex **9**. The hexyl chains and *t*-butyl substituents in **9** are insufficient to impede intermolecular interactions, whereas the mesityl groups of **6** do so. The solution-processed OLEDs reach an EQE of 10% with a maximum luminance of 5400 cd m^{-2} (Dev 5), or EQE of 9.2% with a maximum luminance of 8700 cd m^{-2} (Dev 3). These figures exceed by ~4-fold the values reported for the structurally similar complex **9**, and are the highest values reported for a TADF-based Pt(II) emitter. Moreover, the use of ligand **4** also leads to a significant reduction of the ΔE_{ST} (*e.g.*, to 0.07 eV in **5** in PS, compared to 0.20 eV reported for complex **8**). This is achieved by increasing the T_1 energy in complex **5**.

The high solubility attained using ligand **4** could also be exploited to oxidise the dinuclear Pt(II) **5** complex to the corresponding dinuclear Pt(IV) complex **7**. Analogous attempts to prepare such materials from related, less substituted *NCN–NCN* ligands have led to intractable mixtures, probably due to poor solubility.

In summary, this study has shown how modifying the design of rigid, ditopic, bis-tridentate ligands can simultaneously lead to improvements in several properties of the corresponding Pt_2 complexes, including enhanced solubility, lower propensity to aggregation, and a reduction in ΔE_{ST} that serves to accelerate radiative decay through TADF. We expect TADF to be implicated in the emission of many other 3rd row phosphors and that these findings will help inform the future design of such molecules.

Author contributions

P. P. – Conceptualization, funding acquisition, project administration, formal analysis, investigation (synthesis, photophysics, OLED devices, computations), visualization, writing – original draft, writing – review & editing; Y. M. D. – investigation (synthesis), writing – review & editing; E. V. P. – conceptualization, investigation (synthesis), writing – review & editing; J. A. G. W. – conceptualization, funding acquisition, resources, project administration, supervision, writing – original draft, writing – review & editing.

Data availability

Our supporting research data is available from the Durham Research Online DATAsets Archive (DRO-DATA) open data repository. DOI: **https://doi.org/10.15128/r2tt44pm914**.

Conflicts of interest

There are no conflicts of interest to declare.

Acknowledgements

We thank Dr Dmitry Yufit for determining the structure of compound **7** through X-ray diffraction. P. P. thanks the National Science Centre, Poland for funding under grant no. 2022/47/D/ST4/01496, and the Rector's pro-quality grant, Silesian University of Technology, Poland, grant no: 04/040/RGJ24/0279. E. V. P. and J. A. G. W. acknowledge funding from EPRSC (grant ref. EP/S012788/1). Y. M. D. thanks Durham

**Some deleterious interactions nevertheless remain, as the 3%-loaded devices are generally more efficient than the 5% devices, a trend also widely observed with, for example, Ir(III) emitters.

University Chemistry for partial support of a PhD studentship. P. P. thanks Dr F. B. Dias and Prof. A. P. Monkman for access to facilities. This work made use of the Hamilton High Performance Computing Service of Durham University.

References

1 P. L. dos Santos, P. Stachelek, Y. Takeda and P. Pander, Recent advances in highly-efficient near infrared OLED emitters, *Mater. Chem. Front.*, 2024, **8**, 1731–1766.
2 K. Li, G. S. M. Tong, Q. Wan, G. Cheng, W. Tong, W.-H. Ang, W.-L. Kwong and C. M. Che, Highly phosphorescent platinum(II) emitters: photophysics, materials and biological applications, *Chem. Sci.*, 2016, **7**, 1653–1673.
3 B. Ma, P. I. Djurovich, S. Garon, B. Alleyne and M. E. Thompson, Platinum Binuclear Complexes as Phosphorescent Dopants for Monochromatic and White Organic Light-Emitting Diodes, *Adv. Funct. Mater.*, 2006, **16**, 2438–2446.
4 W. A. Tarran, G. R. Freeman, L. Murphy, A. M. Benham, R. Kataky and J. A. G. Williams, Platinum(II) Complexes of N ∧ C ∧ N-Coordinating 1,3-Bis(2-pyridyl)benzene Ligands: Thiolate Coligands Lead to Strong Red Luminescence from Charge-Transfer States, *Inorg. Chem.*, 2014, **53**, 5738–5749.
5 M. Mauro, A. Aliprandi, D. Septiadi, N. S. Kehr and L. De Cola, When self-assembly meets biology: luminescent platinum complexes for imaging applications, *Chem. Soc. Rev.*, 2014, **43**, 4144–4166.
6 C.-K. Koo, K.-L. Wong, C. W.-Y. Man, Y.-W. Lam, L. K.-Y. So, H.-L. Tam, S.-W. Tsao, K.-W. Cheah, K.-C. Lau, Y.-Y. Yang, J.-C. Chen and M. H.-W. Lam, A Bioaccumulative Cyclometalated Platinum(II) Complex with Two-Photon-Induced Emission for Live Cell Imaging, *Inorg. Chem.*, 2009, **48**, 872–878.
7 P. Wu, E. L. Wong, D. Ma, G. S. Tong, K. Ng and C. Che, Cyclometalated Platinum(II) Complexes as Highly Sensitive Luminescent Switch–On Probes for Practical Application in Protein Staining and Cell Imaging, *Chem. – Eur. J.*, 2009, **15**, 3652–3656.
8 K. Mitra, C. E. Lyons and M. C. T. Hartman, A Platinum(II) Complex of Heptamethine Cyanine for Photoenhanced Cytotoxicity and Cellular Imaging in Near–IR Light, *Angew. Chem., Int. Ed.*, 2018, **57**, 10263–10267.
9 J. Wu, B. Xu, Y. Xu, L. Yue, J. Chen, G. Xie and J. Zhao, Reblooming of the cis -Bis(2-phenylpyridine) Platinum(II) Complex: Synthesis Updating, Aggregation-Induced Emission, Electroluminescence, and Cell Imaging, *Inorg. Chem.*, 2023, **62**, 19142–19152.
10 A. Upadhyay, A. Nepalia, A. Bera, D. K. Saini and A. R. Chakravarty, A Platinum(II) Boron–dipyrromethene Complex for Cellular Imaging and Mitochondria–targeted Photodynamic Therapy in Red Light, *Chem. – Asian J.*, 2023, **18**, 1–11.
11 P. K. Chow, C. Ma, W. P. To, G. S. M. Tong, S. L. Lai, S. C. F. Kui, W. M. Kwok and C. M. Che, Strongly phosphorescent palladium(II) complexes of tetradentate ligands with mixed oxygen, carbon, and nitrogen donor atoms: Photophysics, photochemistry, and applications, *Angew. Chem., Int. Ed.*, 2013, **52**, 11775–11779.
12 M. Yoshida, K. Saito, H. Matsukawa, S. Yanagida, M. Ebina, Y. Maegawa, S. Inagaki, A. Kobayashi and M. Kato, Immobilization of luminescent Platinum(II) complexes on periodic mesoporous organosilica and their water reduction photocatalysis, *J. Photochem. Photobiol., A*, 2018, **358**, 334–344.
13 D. Gómez de Segura, A. Corral-Zorzano, E. Alcolea, M. T. Moreno and E. Lalinde, Phenylbenzothiazole-Based Platinum(II) and Diplatinum(II) and (III) Complexes with Pyrazolate Groups: Optical Properties and Photocatalysis, *Inorg. Chem.*, 2024, **63**, 1589–1606.
14 P. Domingo-Legarda, A. Casado-Sánchez, L. Marzo, J. Alemán and S. Cabrera, Photocatalytic Water-Soluble Cationic Platinum(II) Complexes Bearing Quinolinate and Phosphine Ligands, *Inorg. Chem.*, 2020, **59**, 13845–13857.
15 Y.-C. Wei, S. F. Wang, Y. Hu, L.-S. Liao, D.-G. Chen, K.-H. Chang, C.-W. Wang, S.-H. Liu, W.-H. Chan, J.-L. Liao, W.-Y. Hung, T.-H. Wang, P.-T. Chen, H.-F. Hsu, Y. Chi and P.-T. Chou, Overcoming the energy gap law in near-infrared OLEDs by exciton–vibration decoupling, *Nat. Photonics*, 2020, **14**, 570–577.
16 S.-F. Wang, B.-K. Su, X.-Q. Wang, Y.-C. Wei, K.-H. Kuo, C.-H. Wang, S.-H. Liu, L.-S. Liao, W.-Y. Hung, L.-W. Fu, W.-T. Chuang, M. Qin, X. Lu, C. You, Y. Chi and P.-T. Chou, Polyatomic molecules with emission quantum yields 20% enable efficient organic light-emitting diodes in the NIR(II) window, *Nat. Photonics*, 2022, **16**, 843–850.
17 G. Cheng, P.-K. Chow, S. C. F. Kui, C.-C. Kwok and C.-M. Che, High–Efficiency Polymer Light–Emitting Devices with Robust Phosphorescent Platinum(II) Emitters Containing Tetradentate Dianionic O ∧ N ∧ C ∧ N Ligands, *Adv. Mater.*, 2013, **25**, 6765–6770.
18 Y. Yuan, J. L. Liao, S. F. Ni, A. K. Y. Jen, C. S. Lee and Y. Chi, Boosting Efficiency of Near-Infrared Organic Light-Emitting Diodes with Os(II)-Based Pyrazinyl Azolate Emitters, *Adv. Funct. Mater.*, 2020, **30**, 1–8.
19 H. Yersin, *Highly Efficient OLEDs with Phosphorescent Materials*, Wiley, 2008.
20 P. Pander, R. Daniels, A. V. Zaytsev, A. Horn, A. Sil, T. J. Penfold, J. A. G. Williams, V. N. Kozhevnikov and F. B. Dias, Exceptionally fast radiative decay of a dinuclear platinum complex through thermally activated delayed fluorescence, *Chem. Sci.*, 2021, **12**, 6172–6180.
21 P. Pander, A. V. Zaytsev, A. Sil, J. A. G. Williams, P.-H. Lanoe, V. N. Kozhevnikov and F. B. Dias, The role of dinuclearity in promoting thermally activated delayed fluorescence (TADF) in cyclometallated, N^C^N-coordinated platinum(II) complexes, *J. Mater. Chem. C*, 2021, **9**, 10276–10287.

22 P. Pander, A. V. Zaytsev, A. Sil, J. A. G. Williams, V. N. Kozhevnikov and F. B. Dias, Enhancement of thermally activated delayed fluorescence properties by substitution of ancillary halogen in a multiple resonance-like diplatinum(II) complex, *J. Mater. Chem. C*, 2022, **10**, 4851–4860.

23 H. Uoyama, K. Goushi, K. Shizu, H. Nomura and C. Adachi, Highly efficient organic light-emitting diodes from delayed fluorescence, *Nature*, 2012, **492**, 234–238.

24 Y. Tao, K. Yuan, T. Chen, P. Xu, H. Li, R. Chen, C. Zheng, L. Zhang and W. Huang, Thermally Activated Delayed Fluorescence Materials Towards the Breakthrough of Organoelectronics, *Adv. Mater.*, 2014, **26**, 7931–7958.

25 A. Russegger, S. M. Fischer, A. C. Debruyne, H. Wiltsche, A. D. Boese, R. I. Dmitriev and S. M. Borisov, Tunable Self-Referenced Molecular Thermometers via Manipulation of Dual Emission in Platinum(II) Pyridinedipyrrolide Complexes, *ACS Appl. Mater. Interfaces*, 2024, **16**, 11930–11943.

26 J.-G. Yang, N. Li, J. Li, X.-F. Song, M.-D. Li, J. Zhang and K. Li, A thermally activated delayed fluorescent platinum (II) complex for red organic light emitting diodes with high efficiencies and small roll-off, *J. Mater. Chem. A*, 2024, **12**, 18977–18985.

27 F. Juliá, D. Bautista, J. M. Fernández-Hernández and P. González-Herrero, Homoleptic tris-cyclometalated platinum(IV) complexes: a new class of long-lived, highly efficient ^{3} LC emitters, *Chem. Sci.*, 2014, **5**, 1875–1880.

28 R. J. Ortiz, J. D. Braun, J. A. G. Williams and D. E. Herbert, Brightly Luminescent Platinum Complexes of N ∧ C − ∧ N Ligands Forming Six-Membered Chelate Rings: Offsetting Deleterious Ring Size Effects Using Site-Selective Benzannulation, *Inorg. Chem.*, 2021, **60**, 16881–16894.

29 Y. M. Dikova, D. S. Yufit and J. A. G. Williams, Platinum(IV) Complexes with Tridentate, NNC -Coordinating Ligands: Synthesis, Structures, and Luminescence, *Inorg. Chem.*, 2023, **62**, 1306–1322.

30 S. J. Farley, D. L. Rochester, A. L. Thompson, J. A. K. Howard and J. A. G. Williams, Controlling Emission Energy, Self-Quenching, and Excimer Formation in Highly Luminescent N∧C∧N-Coordinated Platinum(II) Complexes, *Inorg. Chem.*, 2005, **44**, 9690–9703.

31 F. Neese, The ORCA program system, *Wiley Interdiscip. Rev.: Comput. Mol. Sci.*, 2012, **2**, 73–78.

32 F. Neese, Software update: The ORCA program system—Version 5.0, *Wiley Interdiscip. Rev.: Comput. Mol. Sci.*, 2022, **12**, e1606.

33 M. Roemelt, D. Maganas, S. DeBeer and F. Neese, A combined DFT and restricted open-shell configuration interaction method including spin-orbit coupling: Application to transition metal L-edge X-ray absorption spectroscopy, *J. Chem. Phys.*, 2013, **138**, 204101.

34 B. de Souza, G. Farias, F. Neese and R. Izsák, Predicting Phosphorescence Rates of Light Organic Molecules Using Time-Dependent Density Functional Theory and the Path Integral Approach to Dynamics, *J. Chem. Theory Comput.*, 2019, **15**, 1896–1904.

35 R. J. Salthouse, P. Pander, D. S. Yufit, F. B. Dias and J. A. G. Williams, Near-infrared electroluminescence beyond 940 nm in Pt(N^C^N)X complexes: influencing aggregation with the ancillary ligand X, *Chem. Sci.*, 2022, **13**, 13600–13610.

36 S. J. Strickler and R. A. Berg, Relationship between Absorption Intensity and Fluorescence Lifetime of Molecules, *J. Chem. Phys.*, 1962, **37**, 814–822.

37 M. Urban, P. H. Marek-Urban, K. Durka, S. Luliński, P. Pander and A. P. Monkman, TADF Invariant of Host Polarity and Ultralong Fluorescence Lifetimes in a Donor–Acceptor Emitter Featuring a Hybrid Sulfone–Triarylboron Acceptor, *Angew. Chem., Int. Ed.*, 2023, **62**, e202217530.

38 P. Pander, A. V. Zaytsev, L. G. Franca, F. B. Dias and V. N. Kozhevnikov, Unusual Excimer/Dimer Behavior of a Highly Soluble C,N Platinum(II) Complex with a Spiro-Fluorene Motif, *Inorg. Chem.*, 2023, **62**, 18465–18473.

39 P. Pander, A. V. Zaytsev, A. Sil, G. V. Baryshnikov, F. Siddique, J. A. G. Williams, F. B. Dias and V. N. Kozhevnikov, Thermally activated delayed fluorescence in a deep red dinuclear iridium(III) complex: a hidden mechanism for short luminescence lifetimes, *Chem. Sci.*, 2023, **14**, 13934–13943.